Casparian strip diffusion barrier in *Arabidopsis* is made of a lignin polymer without suberin

Sadaf Naseer[a], Yuree Lee[a], Catherine Lapierre[b], Rochus Franke[c], Christiane Nawrath[a], and Niko Geldner[a,1]

[a]Department of Plant Molecular Biology, Biophore, Campus UNIL-Sorge, University of Lausanne, CH-1015 Lausanne, Switzerland; [b]Institut Jean-Pierre Bourgin, Institut National de la Recherche Agronomique-AgroParisTech, Unité Mixte de Recherche 1318, F-78026 Versailles, France; and [c]Ecophysiology of Plants, Institute of Cellular and Molecular Botany, University of Bonn, D-53115 Bonn, Germany

Edited by Philip N. Benfey, Duke University, Durham, NC, and approved May 7, 2012 (received for review April 12, 2012)

Casparian strips are ring-like cell-wall modifications in the root endodermis of vascular plants. Their presence generates a paracellular barrier, analogous to animal tight junctions, that is thought to be crucial for selective nutrient uptake, exclusion of pathogens, and many other processes. Despite their importance, the chemical nature of Casparian strips has remained a matter of debate, confounding further molecular analysis. Suberin, lignin, lignin-like polymers, or both, have been claimed to make up Casparian strips. Here we show that, in *Arabidopsis*, suberin is produced much too late to take part in Casparian strip formation. In addition, we have generated plants devoid of any detectable suberin, which still establish functional Casparian strips. In contrast, manipulating lignin biosynthesis abrogates Casparian strip formation. Finally, monolignol feeding and lignin-specific chemical analysis indicates the presence of archetypal lignin in Casparian strips. Our findings establish the chemical nature of the primary root-diffusion barrier in *Arabidopsis* and enable a mechanistic dissection of the formation of Casparian strips, which are an independent way of generating tight junctions in eukaryotes.

root development | plant nutrition | polarized epithelium

In plants, establishment of a paracellular diffusion barrier is more complex than in animals because it cannot be achieved through direct protein-mediated cell-cell contacts. Instead, establishment of the barrier relies on the coordinated, localized impregnation of the plant cell wall, guided by protein platforms in the plasma membrane of neighboring cells. This very different way of generating a tight junction remains badly understood in molecular terms. The Casparian strips of the endodermis are such localized impregnations of the primary cell wall. The strips render these walls more hydrophobic and resistant to chemical and enzymatic degradation and represent the primary diffusion barrier in young roots. Recently, a family of transmembrane proteins has been identified that is important for the localized deposition of Casparian strips. These Casparian strip membrane domain proteins (CASPs) represent the first proteins to localize to the Casparian strips and, it has been speculated that their function consists in providing a membrane platform for the localized recruitment of polymerizing enzymes (1). For a further mechanistic dissection of Casparian strip formation, it is very important to understand from what kind of polymer early Casparian strips are actually made. Unfortunately, the chemical nature of the Casparian strip polymer has remained a contentious issue for more than a century. Its discoverer, Robert Caspary, pointed out that its resistance to chemical treatments did not allow distinguishing whether it is made of "Holzstoff" (lignin) or "Korkstoff" (suberin) (2). In the following, it was concluded that Casparian strips are made of suberin, an aliphatic polyester that is the main component of cork (3). However, other works found evidence that Casparian strips largely consist of a lignin-like polymer (4). Major current textbooks now describe the Casparian strip as an essentially suberin-based structure (5–8). It is indeed intuitive to assume that Casparian strips are made of suberin because their function as an extracellular (apoplastic) diffusion barrier could be perfectly fulfilled by this hydrophobic polymer. A number of problems have long prevented drawing conclusions about the chemical nature of Casparian strips. First, the ring-like Casparian strips represent only the first stage of endodermal differentiation, which is followed by the deposition of suberin lamellae all around the cellular surface of endodermal cells (secondary stage) (9). Therefore, chemical analysis of whole roots, or even of isolated endodermal tissues, will always find both of the polymers present. Additionally, lignified xylem vessels and suberised/lignified dermal tissues form in close proximity to the endodermis and need to be separated from the Casparian strips for chemical analysis. The few studies that attempted such dissections actually found lignin in Casparian strips, but suberin was also invariably detected (9–11). Natural variation between species could partially explain some of the conflicting results (9, 12). Most importantly, however, there has been a lack of experimental manipulations of suberin and lignin content of the Casparian strips. Only these manipulations could determine which of the polymers is relevant for their functionality as a diffusion barrier. *Arabidopsis*, which allows for precise experimental manipulations, has been absent from most of the older studies, not being a traditional object of botanists. In addition, its very small root system renders chemical analysis and classic histochemical stainings challenging.

Here, we present a precise developmental staging of the appearance of various histochemical stains for suberin and lignin in *Arabidopsis*, using whole-mount staining procedures. This process is combined with functional assays, reporter gene expression analysis, in addition to various pharmacological and novel genetic manipulations of lignin and suberin production. Taken together, our data indicate that, in *Arabidopsis*, suberin is neither present nor required in early Casparian strips, and that the initial endodermal diffusion barrier is made of a lignin polymer.

Results

We had shown previously that the fluorescent dye propidium iodide (PI), widely used to highlight cell walls of *Arabidopsis* roots, can also be used as a convenient apoplastic tracer, the diffusion of which into the inner cell layers of the stele is blocked upon appearance of Casparian strips. PI therefore represents a powerful tool to visualize the presence of a functional endodermal diffusion barrier. Using PI, we compared the cellular distance from the meristem at which the diffusion barrier appears to that of green autofluorescence, indicative of phenolic, lignin-like, compounds and to Fluorol yellow staining, a fluorescent suberin dye (13) (Fig. 1). To our surprise, we observed a radical difference in the onset of the two signals. Although appearance of the green

Author contributions: C.N. and N.G. designed research; S.N., Y.L., C.L., and R.F. performed research; C.N. contributed new reagents/analytic tools; S.N., Y.L., C.L., R.F., and N.G. analyzed data; and S.N. and N.G. wrote the paper.

The authors declare no conflict of interest.

This article is a PNAS Direct Submission.

[1]To whom correspondence should be addressed. E-mail: Niko.Geldner@unil.ch.

This article contains supporting information online at www.pnas.org/lookup/suppl/doi:10.1073/pnas.1205726109/-/DCSupplemental.

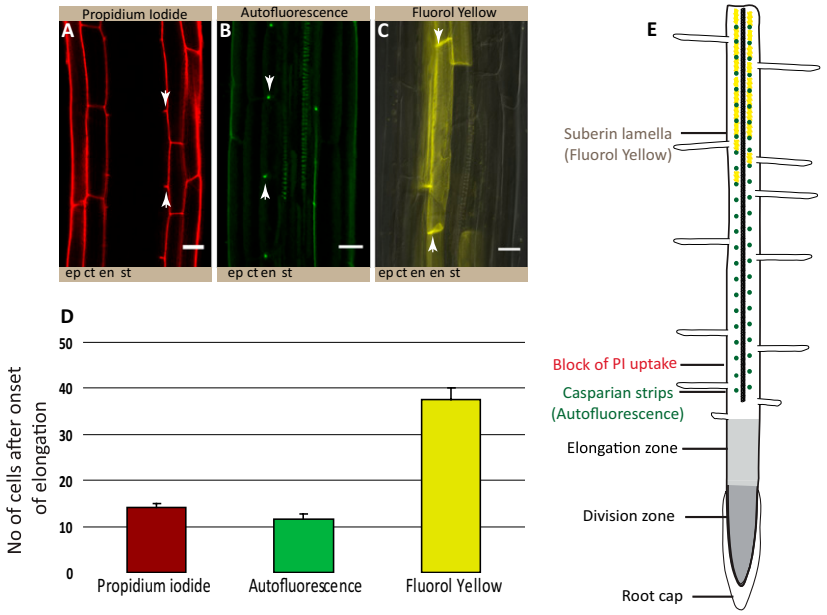

Fig. 1. Lignin, but not suberin stains, correlate with the appearance of the endodermal diffusion barrier. (*A*) Penetration of PI into the stele is blocked at 14.2 ± 0.6 endodermal cells after onset of elongation. (*B*) Dot-like appearance of Casparian strip formation at 11.7 ± 0.9 endodermal cells as visualized by green autofluorescence after clearing. (*C*) Fluorol yellow staining reveals the presence of lamellar suberin on the cellular surface of endodermal cells at 37.5 ± 2.6 endodermal cells. (Scale bars, 20 μm.) (*D*) Quantification of *A*–*C* shows that appearance of green autofluorescence correlates well with block of PI uptake; Fluorol yellow signal appears much later. (*E*) Root schematic showing the different root zones and stages of endodermal differentiation as inferred from *A*–*D*. Stele (st), endodermis (en), cortex (ct), epidermis (ep). *A*–*D*: $n \geq 20$ roots counted per condition. "Onset of elongation" was defined as the zone where an endodermal cell was clearly more than twice its width.

autofluorescence coincided precisely with the block of PI diffusion, Fluorol yellow staining appeared only much later (Fig. 1 *D* and *E*). Moreover, only green autofluorescence appeared as restricted dots in the transversal endodermal cell walls of median, longitudinal optical sections, as would be expected for a Casparian strip signal (Fig. 1*B*). In contrast, Fluorol yellow stain appeared on all cellular surfaces together, and it was impossible to observe a restricted, dot-like staining of the Casparian strip, even in initial stages (Fig. 1*C*). Interestingly, Fluorol yellow appeared in a particular fashion in which individual endodermal cells started to stain very strongly, but neighboring ones did not show any staining. This process led to an initially "patchy" appearance of the suberin stain, which only gradually turned into a continuous signal of endodermal cell files (Fig. 1*C*). We then tested a number of additional histochemical stains for lignin. All of the tested lignin stains showed an early dot-like appearance, coinciding with the block of PI uptake (Fig. S1). Taken together, the data in this analysis pointed to a lignin-like polymer as the initial constituent of Casparian strips and did not support an involvement of suberin. However, it is possible that a stain like Fluorol yellow only detects suberin lamellae, but would not pick up suberin that is associated with lignin in the Casparian strip. To address this possibility, we decided to detect the promoter activities of a number of different suberin biosynthetic genes covering most of the known biosynthetic steps. Essentially all promoter::GUS fusion showed specific activity in the endodermis and all except one displayed a very late and patchy onset of activity (Fig. 2 *A* and *I*), closely matching the appearance of the Fluorol yellow stain (Fig. 2 *J* and *K*). This finding

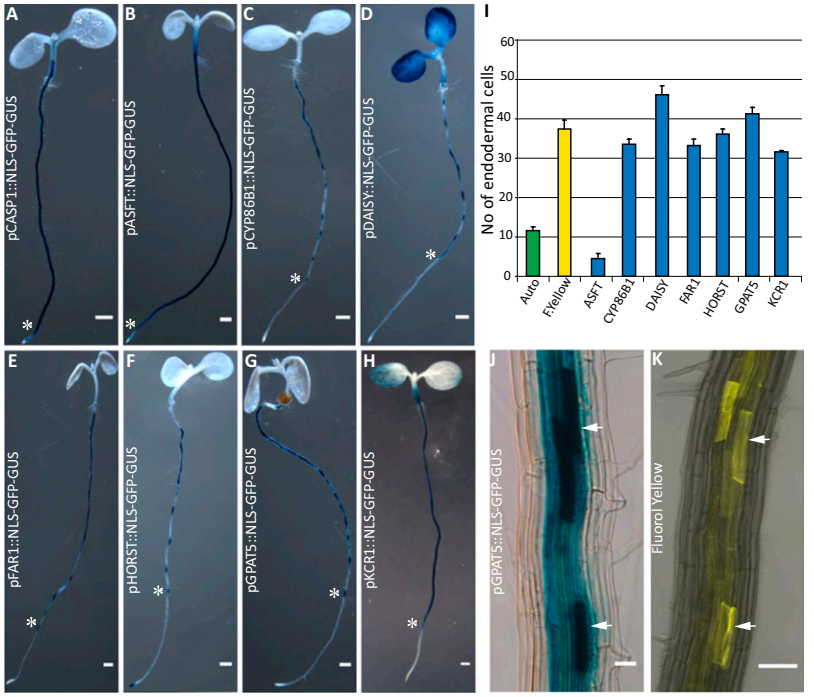

Fig. 2. Suberin biosynthetic genes are turned on after Casparian strip formation. Endodermis-specific Promoter::GUS fusion activity of (*A*) pCASP1::NLS-GFP-GUS, (*B*) pASFT::NLS-GFP-GUS, (*C*) pCYP86B1::NLS-GFP-GUS, (*D*) pDAISY::NLS-GFP-GUS, (*E*) pFAR1::NLS-GFP-GUS, (*F*) pHORST::NLS-GFP-GUS, (*G*) pGPAT5::NLS-GFP-GUS, (*H*) pKCR1::NLS-GFP-GUS; asterisks mark the start of GUS expression. $n = 16$ roots counted. (*I*) Quantifiation of the cellular distance from the meristem at which onset of GUS expression is observed. Appearance of all but one suberin biosynthetic reporter gene coincided well with appearance of Fluorol yellow signals but not with appearance of green autofluorescence. (*J* and *K*) Arrowheads point to patchy GUS-expression pattern (*J*), which matches closely the patterns observed with Fluorol yellow stains (*K*) (Scale bars, 50 μm.)

strongly suggests that Fluorol yellow adequately reports the presence of suberin and that the biosynthetic machinery for suberin is simply not present at the moment of Casparian strip formation. A notable exception among the suberin biosynthetic genes is *ASFT*, which is turned on as early as the *CASP1* promoter and thus slightly precedes formation of Casparian strips (Fig. 2 *A* and *B*, and Fig. S2). ALIPHATIC SUBERIN FERULOYL TRANSFERASE (ASFT) catalyses transfer of ferulic acid onto aliphatic chains (14, 15). On its own, ASFT cannot possibly mediate formation of a suberin polymer, but its early activity could allow the integration of some aliphatic ferulic acid esters into Casparian strips. Finally, we tested whether genetic interference with suberin formation or accumulation had any effect on the presence or functionality of the Casparian strips. Because of redundancy, there are currently no strong, single gene knock-outs of suberin biosynthesis. Nevertheless, we were able to observe a significant delay in the appearance of Fluorol yellow stains in insertion mutants of *HORST*, as well as for other suberin biosynthetic mutants (16) (Fig. 3*A* and Fig. S3). Despite this delay, however, no difference could be observed in the appearance of Casparian strip autofluorescence or block in PI uptake (Fig. 3 *B* and *C*, and Fig. S3).

To obtain a stronger interference with suberin accumulation, we decided to express CUTICLE DESTRUCTION FACTOR 1 (CDEF1), a plant-encoded cutinase (17), under an endodermis-specific promoter. Cutin and suberin show extensive structural similarity, which made it plausible that a cutinase would also effectively degrade suberin. Strikingly, we observed a complete lack of suberin staining in otherwise normal seedling roots in these transgenic lines (Fig. 3*D*). To our knowledge, such a strong, specific interference with suberin accumulation has never been reported and this line will be extremely useful to assess the many supposed physiological roles of suberin in roots. Despite this strong interference with suberin, the appearance of autofluorescent Casparian strips and the PI diffusion barrier remained unaltered (Fig. 3 *E*–*G*). We also observed similar effects by inducible expression of a fungal cutinase (18) (Fig. S4). Thus, our genetic manipulations strongly support the notion that suberin is neither present nor required for the establishment of the Casparian strip diffusion barrier. We then undertook reverse experiments, aimed at specifically blocking lignin biosynthesis. To do so, we used piperonylic acid (PA), targeting an early step in the biosynthesis of monolignols (19). Twenty-four hours of PA treatment does not interfere with continued root growth but clearly affects lignin levels in roots (Fig. S5). However, the treatment led to a dramatic, apparent upward-shift of Casparian strip appearance with respect to the root tip (Fig. 4 *A*–*C* and *E*). This shift results from a block of Casparian strip formation in all newly forming cells. Accordingly, PI penetration was also shifted upwards by a comparable numbers of cells (Fig. 4 *F*, *G*, and *I*). In contrast, the establishment of suberin lamellae was not affected by the treatment (Fig. S6*A*). Exactly the same effects were observed when using a different lignin biosynthetic inhibitor, 2-aminoindan-2-phosphonic acid (AIP) (20) (Fig. S6*B*), acting on a different target in the pathway. Although PA and AIP certainly block monolignol biosynthesis, their early action in the pathway will also lead to a block of other parts of the phenylpropanoid metabolic network. We therefore attempted to complement the inhibitor-induced defects by simultaneous addition of the two canonical components of Angiosperm lignin, coniferyl-, and sinapyl alcohols. Strikingly, the exogenous application of these two compounds allowed the formation of autofluorescent Casparian strips and a functional diffusion barrier, with coniferyl alcohol being the most effective (Fig. 4 *C*–*H* and Fig. S7). This complementation indicates that functional Casparian strips can be made exclusively of the typical monomers found in other lignified tissues, such as xylem vessels.

We then tried to more specifically interfere with monolignol biosynthesis by a genetic approach. This process is very challenging because of the high redundancy within the enzyme families involved (21). However, once a sufficient number of biosynthetic mutants were combined, we expectedly observed pleiotropic germination and growth defects. In independent allelic combinations of a triple and a quintuple insertion mutant, we could nevertheless observe a clear delay in the formation of the PI diffusion barrier (Fig. 4*J* and Fig. S6*C*). Taken together, our results provide strong evidence that the Casparian strip polymer is made from monolignols and that it consists either of conventional lignin or a very similar, lignin-like structure. We therefore sought for ways that would allow a direct chemical analysis of exclusively Casparian strips. Because of the small size of *Arabidopsis* roots, we considered a direct separation of the early Casparian strip network from lignified xylem vessels to be unfeasible. As an alternative, we decided to make use of an *Arabidopsis* mutant, *arabidopsis histidine transfer protein 6* (*ahp6*) (22), which we treated with low amounts of cytokinin. This combination causes strongly delayed xylem differentiation but does not affect formation of Casparian strips (Fig. 5 *A*–*D*). In this way, we generated a root zone, sufficiently long for dissection, that harbors Casparian strips as the only lignified structures. We prepared sufficient material from the first 5 mm of root tips and subjected the samples to thioacidolysis, followed by GC-MS analysis. In this way, we could obtain direct, chemical data on the composition of Casparian strips. As expected, total amount of lignin in these samples was very low. Nonetheless, we were able to unambiguously identify the typical lignin units from their

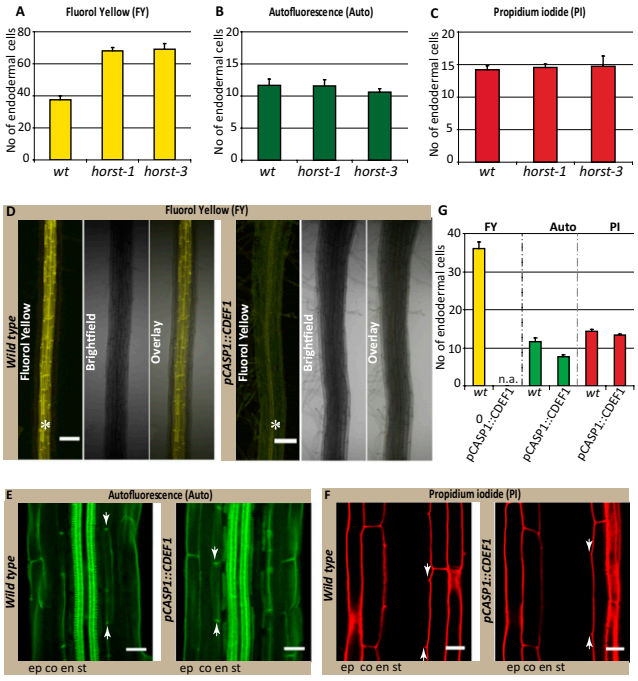

Fig. 3. Suberin degradation has no effect on the formation of functional Casparian strips. (*A*) Fluorol yellow staining reveals significant delay in the appearance of suberin lamellae formation in *horst-1* and *horst-3* insertion lines compared with wild-type (*wt*); (*B*) *horst* mutants do not affect formation of Casparian strips, visualized by autofluorescence. (*C*) Establishment of a functional diffusion barrier, visualized by PI, is also not affected in *horst* mutants. (*D*) No Fluorol yellow signal observed in the *pCASP1::CDEF1* transgenic line, compared with wild-type seedlings; asterisks show the presence (wt, *Left*) and lack of Fluorol yellow signals in endodermis (*Right*). (Scale bar, 100 μm.) (*E*) Casparian strip autofluorescence is not affected by suberin degradation in *pCASP1::CDEF1* transgenic line. (*F*) PI stainings also shows no difference in the formation of a functional diffusion barrier between *pCASP1::CDEF1* and wild-type. *n* = 16 roots counted. (Scale bars *E* and *F*, 20 μm.) (*G*) Quantification of data in *D*–*F*. Stele (st), endodermis (en), cortex (ct), epidermis (ep), not applicable (n.a).

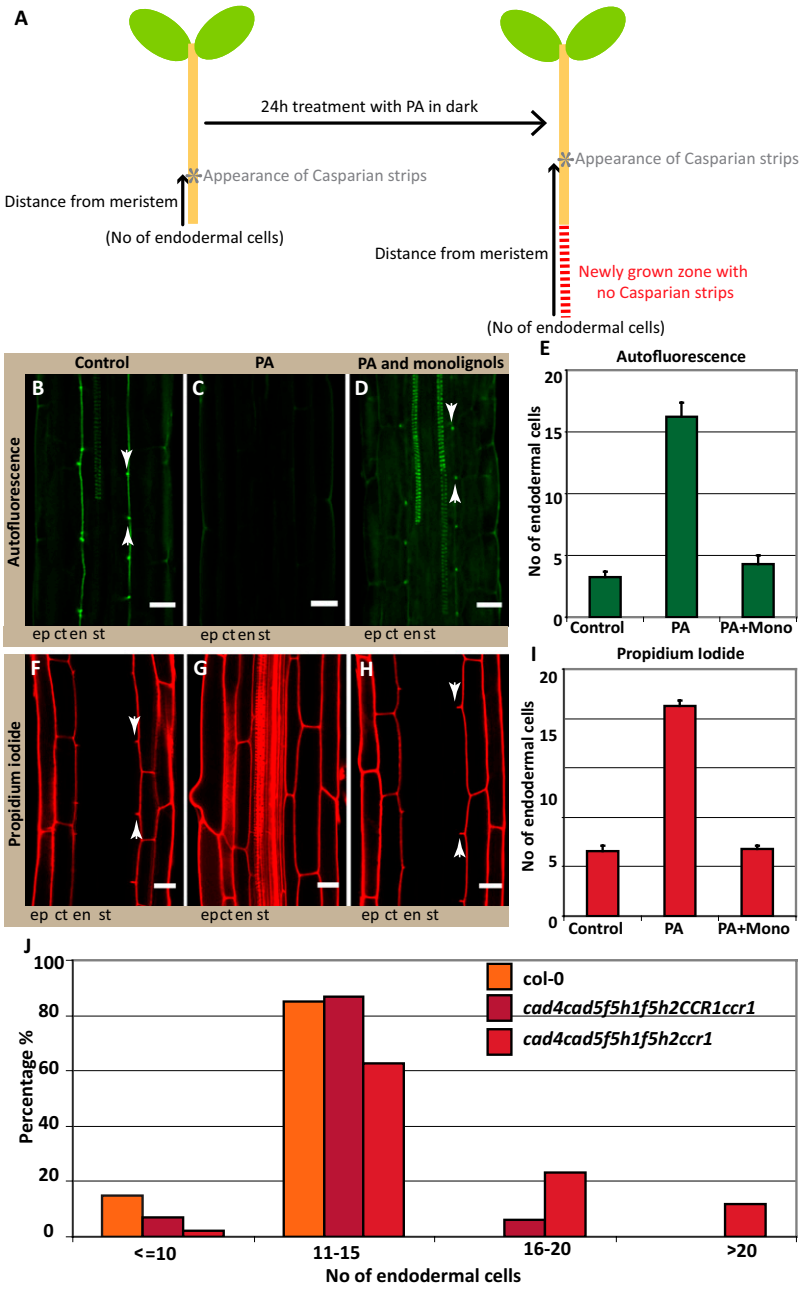

Fig. 4. Interference with monolignol biosynthesis abrogates Casparian strip formation. (*A*) Schematic representation of a seedling explaining how continued root growth after lignin inhibitor treatment results in an apparent "upward shift" of Casparian strip appearance when the cellular distance to the meristem is counted after 24 h. (*B–D*) Autofluorescence after clearing shows the suppression of Casparian strip formation in seedlings treated for 24 h with lignin biosynthesis inhibitor (PA) (*C*), compared with the control (*B*). This effect is complemented by the exogenous application of two monolignols: 20 μM of each coniferyl alcohol and sinapyl alcohol, which allows for the formation of functional Casparian strips (*D*). (*E*) Quantification of *B–D* shows that in the control samples green autofluorescent signal appears around three cells, whereas PA treatment results in the apparent upward-shift of autofluorescent signal to 16 cells, and monolignols complement this inhibitor induced-effect. Signals appear around four cells; close to the control value (*F–H*) PA also blocks the establishment of the diffusion barrier in newly forming cells (*G*) compared with the control (*F*), and this effect is also complemented by monolignol addition (*H*). (*I*) Quantification of *F–H* shows that PA treatment also shifts the block of PI uptake to 21 cells compared with the control samples where PI penetration is blocked around 6 cells. Monolignol addition complements this inhibitor-induced effect and block of PI uptake again appears around 6 cells, matching with the control samples. Arrowheads points to the seventh endodermal cell after onset of elongation. (*J*) Genetic interference using multiple insertion mutants (*ccr1;cad4;cad5;f5h1;f5h2*) of lignin biosynthetic genes reveals a delay in the formation of the diffusion barrier, visualized by PI. In a population of quadruple homozygous (*cad4;cad5;f5h1;f5h2*), segregating for *ccr1*, a delay in the formation of the diffusion barrier is observed in the quadruple mutants, which is further increased in the quintuple mutant. Wild-type (Col): *n* = 60; quadruple mutant *(cad4;cad5;f5h1;f5h2* with *CCR1* either *CCR1/CCR1* or *CCR1/ccr1)*: *n* = 227 and the quintuple mutant *(cad4,cad5,f5h1,f5h2;ccr1)*: *n* = 41. Stele (st), endodermis (en), cortex (ct), epidermis (ep). *B–D* and *F–H*: *n* = 20 roots counted. (Scale bars, 20 μm.)

specific thioacidolysis monomers in ratios that are very similar to that of the xylem-containing wild-type sample (Fig. 5 *E* and *F*). As typical for angiosperm lignin, more than 90% of the monomers in the sample consisted of coniferyl alcohol-derived units, nicely fitting with our exogenous monolignol applications (Fig. 4). Finally, the occurrence of coniferaldehyde end-groups, estimated from

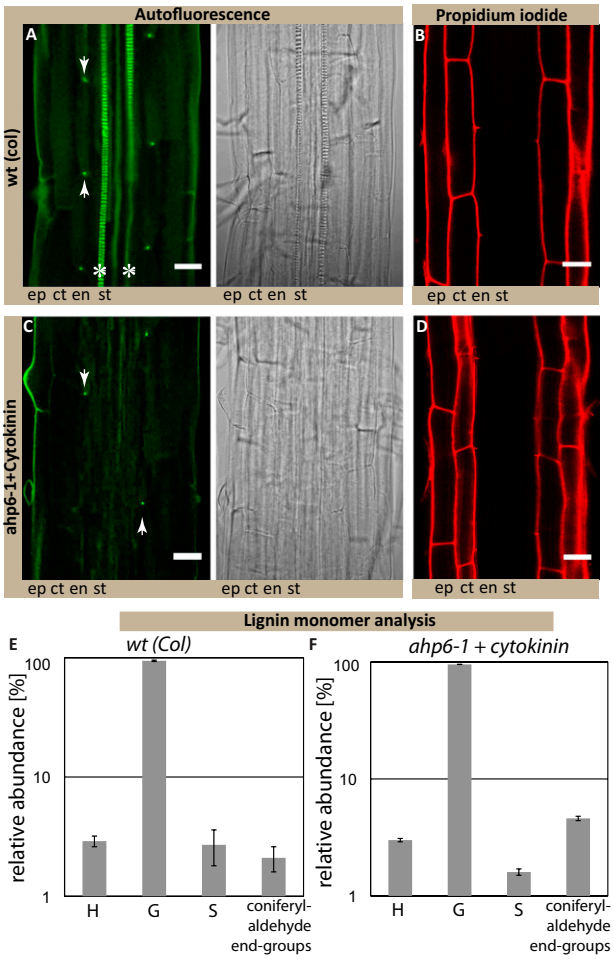

Fig. 5. Casparian strips are made of lignin or a closely related, lignin-like polymer. (*A*) Autofluorescence after clearing shows the appearance of Casparian strip formation (dot-like) and the protoxylem formation. (*B*) PI staining shows functional diffusion barrier. (*C*) Autofluorescence after clearing shows only the dot-like appearance of Casparian strips but no protoxylem formation in *ahp6-1* mutant treated with 10 nM of the cytokinin benzyl-adenine (*ahp6+ck*). (*D*) PI staining confirms presence of a functional diffusion barrier. (Scale bars, 20 μm.) (*E* and *F*) Similar presence and relative abundance of thioacidolysis monomers specifically released from *p*-hydroxyphenyl (H), guaiacyl (G), and syringyl (S) lignin units and from lignin coniferaldehyde end-groups is observed in *wt* (*E*) and *ahp6+ck* root tips (*F*). Total lignin monomers released by thioacidolysis are 208 ± 49 nmol/g for wt and 449 ± 48 nmol/g for *ahp6+ck* root tips. Asterisks mark the presence of xylem vessels in wild-type; arrowheads point to the dot-like structures of the Casparian strips in wt and *ahp6-1*. Stele (st), endodermis (en), cortex (ct), epidermis (ep), wild-type (wt), Cytokinin (ck).

their diagnostic thioacidolysis monomers, fits the phloroglucinol lignin staining observed in Fig. S1*A* and additionally support the idea that genuine lignins are present in the *ahp6* (Casparian strip only) samples. Thus, Casparian strips appear to be made of a polymer that is identical or closely related to the typical lignin found in other cell types in the plant.

Discussion

In summary, our work greatly advances our understanding of the chemical nature and function of Casparian strips. Although it could have been concluded from earlier works that some lignin-like polymer is one of the components of Casparian strips, none of the previous studies did any experimental manipulations that could have established the function and relative importance of lignin and suberin in the Casparian strips. Our work now unambiguously demonstrates that suberin biosynthesis and accumulation occurs much later than the formation of an endodermal barrier and that completely abrogating suberin accumulation still allows the establishment of an efficient barrier to PI penetration. In contrast, monolignol synthesis is absolutely required for establishment of a functional barrier and our reconstitution experiments and chemical analysis both indicate that the Casparian strip is made of lignin or a closely related lignin-like polymer. Our results have important consequences for our thinking about the mechanisms of Casparian strip formation. We can now assume that the localized formation of Casparian strips comes about by confining lignin-polymerizing activity into a meridional ring around the cell. This process could be achieved by localizing lignin-polymerizing enzymes, such as peroxidases or laccases, by confining production of reactive oxygen species or by localized transport of monolignol substrates. The recently identified CASPs are necessary for the correctly localized formation of Casparian strips and appear to form an extensively scaffolded domain within the plasma membrane (the Casparian strip membrane domain, CSD) that precedes and predicts the formation of the Casparian strips themselves. We speculate that the CSD provides a protein platform that allows localization, or localized activation, of the above-mentioned peroxidases/laccases, reactive-oxygen species-producing enzymes, transporters, or combinations of those. Late processes of lignin biosynthesis, such as lignin-polymerization and monolignol transport to the apoplast, remain badly understood. Even more limited is our understanding of the mechanisms that allow the precise subcellular localization of lignin that is seen in many cell types. Our work establishes the endodermis as a promising cellular model for the investigation of lignin formation per se, as well as its subcellular localization. The advantage of the endodermis might be that it is less required for plant survival than xylem vessels, which could be useful for identification and characterization of mutants. In addition, only subsets within the big families of lignin biosynthetic enzymes might be used in the endodermis, which could alleviate problems of redundancy. Finally, the endodermis is a relatively large and peripheral cell layer, compared with many other lignifying tissues. Moreover, it shows a very localized and restricted lignification and stays alive during this process, which should make *in planta* localization studies and cell biological analysis of lignin formation much more straightforward.

Materials and Methods

Plant Material and Growth Conditions. *Arabidopsis thaliana* ecotype Columbia were used for all experiments. For detail of knockout mutants, see Tables S1 and S2. The *ahp6-1* seeds were obtained from Y. Helariutta (University of Helsinki, Helsinki, Finland). Plants expressing the cutinase gene (DEX-CUTE) were generated by a dexamethasone-inducible promoter (18, 23). Plants were germinated on 1/2 MS (Murashige and Skoog) agar plates after 2 d in dark at 4 °C. Seedlings were grown vertically in Percival chambers at 22 °C, under long days (16-h light/8-h dark), and were used at 5 d after shift to room temperature.

Chemicals. PI was purchased from Invitrogen. AIP was kindly provided by Jerzy Zon (Wroclaw Technical University, Wroclaw, Poland). All other dyes, inhibitors, solvents, and chemicals were purchased from Sigma-Aldrich.

Microscopy, Histology, and Quantitative Analysis. Confocal laser scanning microscopy was performed on an inverted Leica SP2 or Zeiss LSM 700 confocal microscope. Excitation and detection windows were set as follows: GFP 488 nm, 500–600 nm; PI 488 nm, 500–550 nm. Autofluorescence and Fluorol yellow were detected with standard GFP filter under wide-field microscope (Leica DM5500). Fluorol yellow staining was performed according to ref. 13. Casparian strips were visualized, as described in refs. 24 and 25. For visualization of the apoplastic barrier, seedlings were incubated in the dark for 10 min in a fresh solution of 15 μM (10 μg/mL) PI and rinsed two times in water (24). For quantification, "onset of elongation" was defined as the point where an endodermal cell in a median optical section was more than twice its width. From this point, cells in the file were counted until the respective signals were detected, see also ref. 24.

Inhibitor Assays. For lignin inhibitor assays, 5-d-old seedlings were incubated in 10 μM PA or 50 μM AIP for 24 h in dark and washed with 1/2 MS before histochemical analysis.

Lignin Quantification. Lignin content in roots was determined by the thioglycolic extraction method as described in ref. 26. The absorbance was measured at 280 nm, lignin alkali (Sigma-Aldrich) was used for generation of a standard.

Evaluation of Lignin Level and Composition in Root Tips by Thioacidolysis. Lignin structure was evaluated by thioacidolysis performed from 6 to 25 mg of the collected samples (air-dried, duplicate experiments). Samples were collected from 5-d-old seedlings. For *Columbia* and cytokinin-treated *ahp6* roots, ~200 mg fresh weight from the first 5 mm of root tips were collected, as the zone that contained no xylem vessels in *ahp6*. Samples were subjected to thioacidolysis, together with 0.083 mg of C21 and 0.12 mg C19 internal standards. After the reaction, the lignin-derived monomers were extracted as usually done (27), the combined organic extracts were concentrated to about 0.2 mL and then 10 μL of the sample were silylated by 50 μL BSTFA and 5 μL pyridine before injection onto a DB1 supelco capillary columns (carrier gas helium, constant flow rate 1 mL/min) operating from 40 to 180 °C at +30 °C/min, then 180–260 °C at +2 °C/min and combined to an ion-trap mass spectrometer (Varian Saturn2100) operating in the electron impact mode (70 eV), with ions detected on the 50–600 *m/z* range. The surface area of the internal standard peaks, measured on reconstructed ion chromatograms [at *m:z* (57+71+85)] and the surface area of the H, G, and S monomers (measured at *m/z* 239, 269, and 299 respectively), were measured.

Vector Construction and Transgenic Lines. For cloning and generation of expression constructs, Gateway Cloning Technology (Invitrogen) was used. For primer details, see Tables S1–S3. Transgenic plants were generated by introduction of the plant expression constructs into a pSOUP containing *Agrobacterium tumefaciens* strain GV3101. Transformation was done by floral dipping (28).

GUS-Staining. For promoter::GUS analysis, 5-d-old seedling were incubated in 5-bromo-4-chloro-3-indolyl-β-D-glucuronide (X-Gluc) staining buffer solution (10 mM EDTA, 0.1% Triton X-100, 2 mM Fe2+CN, 2 mM Fe3+CN, 1 mg/mL X-Gluc) in 50 mM sodium phosphate buffer (pH7.2) at 37 °C for 3~5 h in darkness.

Generation and Analysis of Multiple Monolignol Biosynthesis Mutants. For generation of quintuple monolignol mutants, T-DNA insertion lines from the SALK or GABI-KAT collection were used (all in Columbia). Analysis was done on a quadruple mutant, segregating for *ccr1*. Each seedling was analyzed for the cellular distance from the meristem at which PI diffusion becomes blocked. The same seedlings were then transferred to soil and genotyped. The results were confirmed in an independent crossing in which all alleles (except *ccr1*) were different. In this second cross, *CAD4* and *CAD5* insertion mutants were from the Versailles collection (in Wassilewskija). Here, a *cad5 ccr1* double mutant, segregating for *cad4*, was analyzed as above. See Tables S1 and S2 for additional information.

ACKNOWLEDGMENTS. We thank Dr. J. Zon for providing 2-aminoindan-2-phosphonic acid; Y. Helariutta for *ahp6* seeds; L. Jouanin for the ccc triple mutant; Nicolaus Amrhein for sharing unpublished results; E. Pesquet for proposing the mono-lignol complementation experiments; F. Beisson, Y. Li-Beisson, and Lukas Schreiber for discussions and sharing of material; and J. Alassimone, D. Roppolo, and J. Vermeer for critically reading the manuscript. This work was funded by a European Research Council Young Investigator grant and grants from the Swiss National Science Foundation (to N.G.), and a European Molecular Biology Organization long-term fellowship (to Y.L.).

1. Roppolo D, et al. (2011) A novel protein family mediates Casparian strip formation in the endodermis. *Nature* 473:380–383.
2. Caspary R (1865) Remarks on the protective sheath and the formation of stem and root (translated from German). *Jahrbücher für wissenschaftliche Botanik* 4:101–124.
3. Espelie KE, Kolattukudy PE (1979) Composition of the aliphatic components of suberin of the endodermal fraction from the first internode of etiolated sorghum seedlings. *Plant Physiol* 63:433–435.
4. Vanfleet DS (1961) Histochemistry and function of the endodermis. *Bot Rev* 27: 165–220.
5. Taiz L, Zeiger E (2006) *Plant Physiology* (Sinauer Associates, Sunderland, MA), 4th Ed.
6. Esau K (1977) *Anatomy of Seed Plants* (Wiley, New York), 2nd Ed.
7. Raven PH, Evert RF, Eichhorn SE (2005) *Biology of Plants* (W.H. Freeman, New York), 7th Ed.
8. Hopkins WG (1999) *Introduction to Plant Physiology* (J. Wiley, New York), 2nd Ed.
9. Schreiber L, Hartmann K, Skrabs M, Zeier J (1999) Apoplastic barriers in roots: Chemical composition of endodermal and hypodermal cell walls. *J Exp Bot* 50: 1267–1280.
10. Zeier J, Ruel K, Ryser U, Schreiber L (1999) Chemical analysis and immunolocalisation of lignin and suberin in endodermal and hypodermal/rhizodermal cell walls of developing maize (*Zea mays* L.) primary roots. *Planta* 209:1–12.
11. Zeier J, Schreiber L (1997) Chemical composition of hypodermal and endodermal cell walls and xylem vessels isolated from *Clivia miniata* (Identification of the biopolymers lignin and suberin). *Plant Physiol* 113:1223–1231.
12. Wilson CA, Peterson CA (1983) Chemical-composition of the epidermal, hypodermal, endodermal and intervening cortical cell-walls of various plant-roots. *Ann Bot (Lond)* 51:759–769.
13. Lux A, Morita S, Abe J, Ito K (2005) An improved method for clearing and staining free-hand sections and whole-mount samples. *Ann Bot (Lond)* 96:989–996.
14. Molina I, Li-Beisson Y, Beisson F, Ohlrogge JB, Pollard M (2009) Identification of an *Arabidopsis* feruloyl-coenzyme A transferase required for suberin synthesis. *Plant Physiol* 151:1317–1328.
15. Gou J-Y, Yu X-H, Liu C-J (2009) A hydroxycinnamoyltransferase responsible for synthesizing suberin aromatics in *Arabidopsis*. *Proc Natl Acad Sci USA* 106:18855–18860.
16. Höfer R, et al. (2008) The *Arabidopsis* cytochrome P450 CYP86A1 encodes a fatty acid omega-hydroxylase involved in suberin monomer biosynthesis. *J Exp Bot* 59: 2347–2360.
17. Takahashi K, et al. (2010) Ectopic expression of an esterase, which is a candidate for the unidentified plant cutinase, causes cuticular defects in *Arabidopsis* thaliana. *Plant Cell Physiol* 51:123–131.
18. Chassot C, Nawrath C, Métraux JP (2007) Cuticular defects lead to full immunity to a major plant pathogen. *Plant J* 49:972–980.
19. Schalk M, et al. (1998) Piperonylic acid, a selective, mechanism-based inactivator of the trans-cinnamate 4-hydroxylase: A new tool to control the flux of metabolites in the phenylpropanoid pathway. *Plant Physiol* 118:209–218.
20. Amrhein N, Frank G, Lemm G, Luhmann HB (1983) Inhibition of lignin formation by L-alpha-aminooxy-beta-phenylpropionic acid, an inhibitor of phenylalanine ammonia-lyase. *Eur J Cell Biol* 29:139–144.
21. Thévenin J, et al. (2011) The simultaneous repression of CCR and CAD, two enzymes of the lignin biosynthetic pathway, results in sterility and dwarfism in *Arabidopsis thaliana*. *Mol Plant* 4:70–82.
22. Mähönen AP, et al. (2006) Cytokinin signaling and its inhibitor AHP6 regulate cell fate during vascular development. *Science* 311:94–98.
23. Aoyama T, Chua NH (1997) A glucocorticoid-mediated transcriptional induction system in transgenic plants. *Plant J* 11:605–612.
24. Alassimone J, Naseer S, Geldner N (2010) A developmental framework for endodermal differentiation and polarity. *Proc Natl Acad Sci USA* 107:5214–5219.
25. Malamy JE, Benfey PN (1997) Organization and cell differentiation in lateral roots of *Arabidopsis thaliana*. *Development* 124:33–44.
26. Bruce RJ, West CA (1989) Elicitation of lignin biosynthesis and isoperoxidase activity by pectic fragments in suspension cultures of castor bean. *Plant Physiol* 91:889–897.
27. Lapierre C, et al.; De Nadai V (1999) Structural alterations of lignins in transgenic poplars with depressed cinnamyl alcohol dehydrogenase or caffeic acid O-methyltransferase activity have an opposite impact on the efficiency of industrial kraft pulping. *Plant Physiol* 119:153–164.
28. Clough SJ, Bent AF (1998) Floral dip: A simplified method for *Agrobacterium*-mediated transformation of *Arabidopsis thaliana*. *Plant J* 16:735–743.